Figure 8 Small industrial-scale centrifuge for dewatering fresh-cut produce. The machine is operated in batch mode, but use of insertable plastic bowl minimizes down time between loads. Reproduced with permission from Freshline Machines, Sydney, Australia.

separations such as dewatering of vegetables. Performance demands also vary widely, ranging from high **g** applications required in isolating and manufacturing the diverse products of biotechnology to dewatering hundreds of tons of municipal sewage per day using machines of relatively low **g** capability. This is made possible by the wide variety of machines available. The recent application of decanters as press replacements in the fruit and vegetable juice industry required the independent development and widespread use of pectin-digesting enzymes (pectinases) for routine juice production. The reduction in viscosity and release of dense core particles from the fruit mash which is characteristic of the action of these enzymes is a necessary precondition for the successful use of decanters. The fruit-processing industry is increasingly interested in the production of products from new, unconventional fruits and vegetables. An example is sea buckthorn, a fruit which consists of a seed, pulp and pulp oil, a three-phase system which might be separated into an oil stream, a stable opalescent juice and a seed containing pulpy ejecta in a single operation using a three-phase decanter. From these two examples drawn from the author's experiences in this industry it appears that future innovations are likely to be applications, which will in turn drive further refinement and development of the centrifugal machinery.

See also: **II/Centrifugation:** Theory of Centrifugation.

Further Reading

Beveridge T (1997) Juice extraction from apples and other fruits and vegetables. *Critical Review of Food Science and Nutrition* 37: 449–469.

Brunner KH and Hemfort H (1988) Centrifugal separation in biotechnological processes. In: Mizrahi A (ed.) *Downstream Processes: Equipment and Techniques. Advances in Biotechnological Processes*, vol 8, pp. 1–50. New York: Alan R. Liss.

Dahlstrom DA, Bennett RC, Emmett RC *et al.* (1997) Liquid–solid operations and equipment: centrifuges. In: Perry RH, Green DW and Maloney JO (eds) *Perry's Chemical Engineers' Handbook*, 7th edn, pp. 18–106. New York, NY: McGraw-Hill.

Leung WW-F (1998) *Industrial Centrifugation Technology*. New York: McGraw-Hill.

White WF (1979) Centrifuges. In: Bhatia MV and Cheremisinoff PN (eds) *Solids Separation and Mixing*. Process Equipment Series, vol. 1, p. 81. Westport CT: Technomic.

Whittington PN (1990) Fermentation broth clarification techniques. *Applied Biochemistry and Biotechnology* 23: 91–121.

DropBooks

Macromolecular Interactions: Characterization by Analytical Ultracentrifugation

D. J. Winzor, Department of Biochemistry, University of Queensland, Brisbane, Australia

Copyright © 2000 Academic Press

Analytical ultracentrifugation refers to the analysis of a macromolecular solution by its subjection to gravitational forces up to 300 000-fold greater than gravity. From its inception by Svedberg in the mid-1920s, analytical ultracentrifugation has played a leading role in studies of macromolecular systems. One early success was its demonstration that proteins were polypeptides of discrete length rather than

polydisperse polymers of amino acid residues – the popular concept amongst colloid chemists at that time. This revolutionary finding was the seminal contribution that generated the present-day fields of protein chemistry and molecular biology. Indeed, for 40 years, the analytical ultracentrifuge was the primary source of information on the molecular mass and heterogeneity of proteins, as well as on the polydispersity of polymer preparations. At that stage, preparative ultracentrifugation, gel permeation (size exclusion) chromatography and gel electrophoresis were developed to take advantage of macromolecular separation on the basis of size and shape (as well as charge in some forms of gel electrophoresis). Meanwhile, the sedimentation equilibrium variant of analytical ultracentrifugation retained supremacy for many years as the benchmark standard of molecular mass measurement for a homogeneous protein – a role now being taken over by mass spectrometry. Furthermore, inroads into its status as the method of choice for determining molecular size distributions for polydisperse polymer preparations have now been made by light scattering as the means of analysing the column eluate in gel permeation chromatography. Nevertheless, such is the strength of analytical ultracentrifugation that it has survived those losses of traditional roles to become an invaluable tool for the characterization of reversible macromolecular interactions – a task which is beyond most of the techniques that have usurped its traditional roles.

Many proteins comprise a mixture of monomeric and polymeric states that coexist in rapid association equilibrium, whereupon the relative proportions of the two macromolecular states vary with total solute concentration in accordance with Le Chatelier's principle: the polymeric state is favoured by an increase in solute concentration whereas monomer is favoured by dilution. Analytical ultracentrifugation has great potential for characterizing the self-association equilibrium by virtue of these concentration-dependent changes in the average macromolecular state of the solute, and also for the characterization of rapid equilibria involving dissimilar reactants, for which similar considerations apply. The main emphasis in current analytical ultracentrifugation is thus the study of noncovalent macromolecular association equilibria: protein–protein interactions such as those involved in enzyme self-association or the binding of an antibody to its eliciting protein antigen; and protein–nucleic acid interactions such as those associated with regulation of the transcription of genetic information.

Sedimentation Velocity and Sedimentation Equilibrium

A complex in rapid association equilibrium with reactant species has no separate existence in the absence of the reactants. The characterization of such interactions requires methods that can accommodate the equilibrium coexistence of several species. This requirement is readily accommodated by either of the commonly used techniques in analytical ultracentrifugation – sedimentation velocity and sedimentation equilibrium. In the former, the centrifuge is operated at a sufficiently high angular velocity (speed) for the centrifugal force on a solute to dominate its migration. In sedimentation equilibrium the same instrument is operated at a much lower angular velocity to effect a balance between the radially outward flux of solute and the back-diffusional flow in response to the concentration gradient being generated. Before considering their application to the characterization of interacting systems, it is appropriate to describe the two techniques in relation to the information derived for a single noninteracting solute.

Measurement of a Sedimentation Coefficient

In sedimentation velocity, a solution is placed in a sector-shaped cell which allows unimpeded migration of solute molecules in a radially outward direction in response to the applied centrifugal field. At the commencement of the experiment, the solute concentration is uniform throughout the cell, but the application of a strong centrifugal field (typically 200 000–300 000 g operating at 50 000–60 000 rpm) leads to a progressive removal of solute from the inner region of the cell (**Figure 1**).

Migration of the resultant solute boundary is recorded optically and the sedimentation coefficient of the solute, s_A, is then determined from the rate of migration. Specifically:

$$s_A = (dr_p/dt)/\omega^2 r) = (d \ln r_p)/dt)/\omega^2 \qquad [1]$$

where r_p denotes the radial position (cm) of the solute boundary after centrifugation at angular velocity ω (rad s^{-1}) for time t (s). Traditionally, the sedimentation coefficient has thus been determined from the slope ($\omega^2 s_A$) of the time dependence of $\ln r_p$. Despite being the rate of migration per unit field, s_A has the dimensions of time, but is usually reported in Svedberg units S ($1\ S = 10^{-13}$ s).

At the limit of zero solute concentration, the sedimentation coefficient, s^o_A, is related to molecular

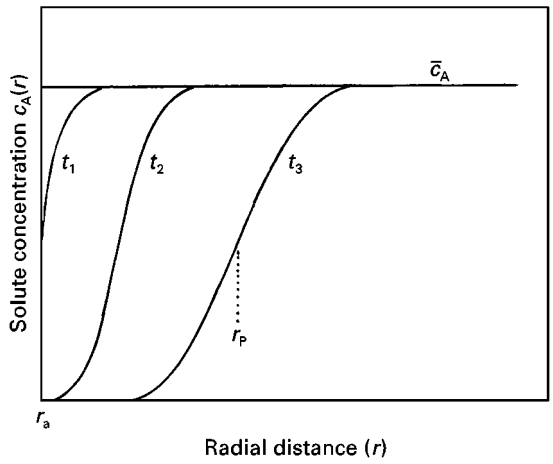

Figure 1 Schematic representation of migration in a sedimentation velocity experiment, showing the generation of a boundary between solvent and the solution subjected to centrifugation: r_p denotes the mean boundary position at time t_3, and r_a the air–liquid meniscus (boundary position at zero time).

parameters by the expression:

$$s^o_A = M_A(1 - \bar{\nu}_A\rho_s)/Nf_A) \qquad [2]$$

where f_A denotes the shape-dependent translational frictional coefficient of the solute with molecular mass M_A and partial specific volume $\bar{\nu}_A$: ρ_s is the solvent density and N is Avogadro's number. Elimination of the frictional coefficient on the assumption of spherical geometry for the solute ($f_A = 6\pi\eta_s a_A$) leads to the relationship:

$$s^o_A = M_A(1 - \bar{\nu}\rho_s)/(6\pi\eta_s a_A) \qquad [3]$$

where η_s is the solvent density and a_A is the Stokes radius of the solute (radius of the equivalent hydrodynamic sphere). The sedimentation coefficient is thus a function of the size (shape) as well as the buoyant molecular mass, $M_A(1 - \bar{\nu}_A\rho_s)$, of the solute.

Experimental Aspects of Sedimentation Equilibrium

Unequivocal determination of the buoyant molecular mass by analytical ultracentrifugation is clearly conditional upon replacement of the frictional coefficient in eqn [2]. On the grounds that the translational diffusion coefficient, D^o_A, is related to f_A by the expression:

$$D^o_A = RT/(Nf_A) \qquad [4]$$

where R and T refer to the universal gas constant and the absolute temperature (K), respectively, the influence of f_A upon the separate magnitudes of the sedimentation and diffusion coefficients disappears from their ratio. Thus:

$$s^o_A/D^o_A = M_A(1 - \bar{\nu}_A\rho_s)/(RT) \qquad [5]$$

In sedimentation equilibrium, the solute distribution is governed by this ratio of s^o_A/D^o_A. The parameter to emerge from the analysis of such distributions is the buoyant molecular mass of the solute, $M_A(1 - \bar{\nu}_A\rho_s)$. Its conversion to a molecular mass requires assignment of a magnitude to $(1 - \bar{\nu}_A\rho_s)$, which may be determined experimentally by density measurements and the relationship $(1 - \bar{\nu}_A\rho_s) \approx (\rho - \rho_s)/c_A$, where ρ is the density of a solute solution with weight concentration c_A.

Sedimentation equilibrium experiments are conducted in a double-sector cell. One sector contains the solution of macromolecular solute and the other the appropriate solvent, which for charged solutes is the buffer with which the solution of macro-ion is in dialysis equilibrium. As in sedimentation velocity, the solute concentration is initially uniform throughout the column of solution (**Figure 2**). Application of the centrifugal field then results in depletion of solute in the vicinity of the air–liquid meniscus (r_a) and its accumulation at the cell base (r_b). However, at the relatively low speeds of such experiments (say, 10 000 rpm for a 50 kDa protein), these tendencies are countered by back-diffusion in response to the concentration gradient being formed. The net result is a progression towards

DropBooks

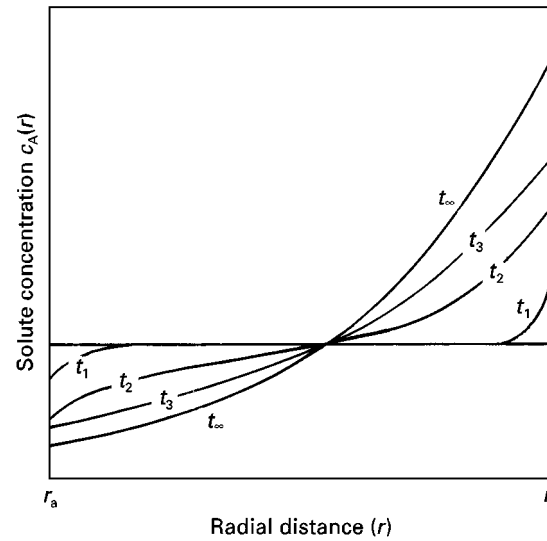

Figure 2 Schematic representation of the approach to a time-independent distribution in a sedimentation equilibrium experiment: the initially uniform concentration gradually changes into an exponential distribution described by eqn [7] for a single solute.

a time-independent exponential increase in solute concentration across the cell (**Figure 2**).

Because the time taken to attain sedimentation equilibrium varies inversely with the square of the column length, columns longer than 3 mm are rarely used. Whereas 3–4 weeks of centrifugation would be required to attain time independence of the solute distribution in a completely filled cell ($r_b - r_a \approx 1$ cm), effective sedimentation equilibrium can be reached within 16–36 h by decreasing the column length to 2–3 mm.

In the original treatise on analytical ultracentrifugation published by Svedberg and Pedersen in 1940, sedimentation equilibrium was considered in terms of the balance between the processes of sedimentation and diffusion. However, later consideration led to the realization that results from such experiments were amenable to rigorous thermodynamic analysis by expressing the diffusional flow in terms of the negative gradient of solute chemical potential. Consequently, even though the experimental record is in terms of solute concentration as a function of radial distance, the distribution of a single solute at sedimentation equilibrium is defined in terms of its thermodynamic activity:

$$z_A(r) = z_A(r_F)\exp[M_A(1-\bar{\nu}_A\rho_s)\omega^2(r^2-r_F^2)/(2RT)] \quad [6]$$

which relates the thermodynamic activity of solute at any given radius, $z_A(r)$, to that at a chosen reference radial position, r_F. Although procedures have now been devised which make allowance for effects of thermodynamic nonideality, the situation is simplified for the present purpose by restricting consideration to ideal systems in which the two thermodynamic activities may be replaced by concentrations $c_A(r)$ and $c_A(r_F)$: eqn [6] thus becomes:

$$c_A(r) = c_A(r_F)\exp[M_A(1-\bar{\nu}_A\rho_s)\omega^2(r^2-r_F^2)/(2RT)] \quad [7]$$

From the logarithmic form of eqn [7] namely:

$$\ln c_A(r) = \ln c_A(r_F) + M_A(1-\bar{\nu}_A\rho_s)\omega^2(r^2-r_F^2)/(2RT) \quad [8]$$

it is evident that:

$$M_A(1-\bar{\nu}_A\rho_s) = (2RT/\omega^2)\mathrm{d}[\ln c_A(r)]/\mathrm{d}r^2 \quad [9]$$

which allows an unequivocal estimate of the buoyant molecular mass to be obtained from the slope of $\ln c_A(r)$ versus the square of radial distance.

Ultracentrifuge Studies of Solute Self-association

The use of analytical ultracentrifugation in protein chemistry for molecular mass determination is now usually bypassed in favour of its calculation from the amino acid sequence or its measurement by mass spectrometry. However, because such molecular mass values refer only to the covalently linked polypeptides chain(s), they provide no information about the macromolecular state of the functional protein or enzyme. In the simplest current application of sedimentation equilibrium, molecular mass measurement is sometimes used to elucidate the nature of quaternary structure, which is an example of a self-association equilibrium displaced completely in favour of the polymeric state.

The aim of this section is to outline the basic principles of the use of analytical ultracentrifugation for the characterization of reversibly associating systems. Although more elaborate and intricate procedures are employed in practice, their description is beyond the scope of this introduction to the topic.

Characterization of Solute Self-association by Sedimentation Velocity

Because of the concentration-dependent variation in the average macromolecular state of a self-associating solute, the best approach in sedimentation velocity studies is to determine the dependence of the weight-average sedimentation coefficient, $\bar{s}_A$, upon total solute concentration, $\bar{c}_A$. Procedural details for the measurement of $\bar{s}_A$ are as described above (eqn [1]), except that the asymmetric shape of the single reaction boundary that forms between solvent and the plateau region with concentration $\bar{c}_A$ (**Figure 1**) necessitates the location of the boundary position, $\bar{r}_p$, as the square root of the second moment:

$$\bar{r}_p^2 = \left[\int_0^{\bar{c}_A} r^2 \mathrm{d}\bar{c}_A\right]/\bar{c}_A \quad [10]$$

to make allowance for the effects of migration in a sector-shaped cell rather than one with uniform cross-sectional area.

For a two-state self-association involving monomer (species 1) and dimer (species 2) the weight-average sedimentation coefficient is given by the expression:

$$\bar{s}_A = \alpha_1 s_1 + (1-\alpha_1)s_2 \quad [11]$$

where $\alpha_1 = c_1/\bar{c}_A$ is the weight fraction of monomer, and where the sedimentation coefficient of

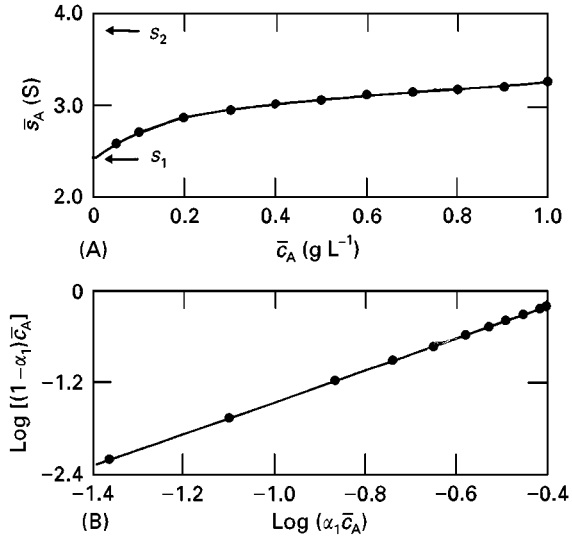

Figure 3 Studies of solute self-association by sedimentation velocity: (A) Concentration dependence of the weight-average sedimentation coefficient simulated (eqn [10]) for a monomer–dimer system where $K_2 = 3.5$ L g^{-1}, $s_1 = 2.4$ S and $s_2 = 3.8$ S. (B) Analysis of the data for the determination of K_2 by means of eqn [13].

monomer, s_1, may be obtained by extrapolation of $\bar{s}_A$ to zero solute concentration (**Figure 3A**). However, the evaluation of α_1 from eqn [11] also depends upon knowledge of s_2, the sedimentation coefficient of dimer, which is not readily obtained experimentally. An estimate is therefore usually made on the basis of the relationship $s_2 = s_1(2^{2/3})$, which follows from eqn [3] and assumed spherical geometry for monomeric and dimeric species. Knowledge of s_2 then allows evaluation of the weight fraction of monomer from the following rearrangement of eqn [11]:

$$\alpha_1 = (s_2 - \bar{s}_A)/(s_2 - s_1) \qquad [12]$$

whereupon the dimerization constant, $K_2 = (1 - \alpha_1)\bar{c}_A/(\alpha_1\bar{c}_A)^2$, may be determined.

Application of this approach to the data in **Figure 3A**, which have been simulated for a system with $s_1 = 2.4$ S, $s_2 = 3.8$ S and $K_2 = 3.5$ L g^{-1}, is illustrated in **Figure 3B**. From the logarithmic form of the expression for the dimerization constant ($K_2 = c_2/c_1^2$), namely:

$$\log[(1 - \alpha_1)c_A] = \log K_2 + 2\log(\alpha_1\bar{c}_A) \qquad [13]$$

in present terminology, K_2 may be obtained as the ordinate intercept of the linear dependence of $\log[(1 - \alpha_1)\bar{c}_A]$ versus $\log(\alpha_1\bar{c}_A)$; this has a mandatory slope of 2 for a monomer–dimer equilibrium.

Characterization of Solute Self-association by Sedimentation Equilibrium

The above approach can be applied to the dependence of weight-average molecular mass $\bar{M}_A$ upon total solute concentration $\bar{c}_A$ by substituting molecular masses for the corresponding sedimentation coefficients in eqn [12]. Furthermore, there is no ambiguity about the magnitude of M_2, which is twice the value of $\bar{M}_A$ in the limit of zero solute concentration. Although this was indeed the original procedure used for characterizing solute self-association by sedimentation equilibrium, it has been superseded by a more accurate method involving direct analysis of the sedimentation equilibrium distribution(s).

Figure 4A presents simulated sedimentation equilibrium distributions at 15 000 and 25 000 rpm for a reversibly dimerizing protein with a buoyant molecular mass of 6.5 kDa for monomer ($M_1 \approx 25$ kDa) and an equilibrium constant of 3.5 L g^{-1}. Because the

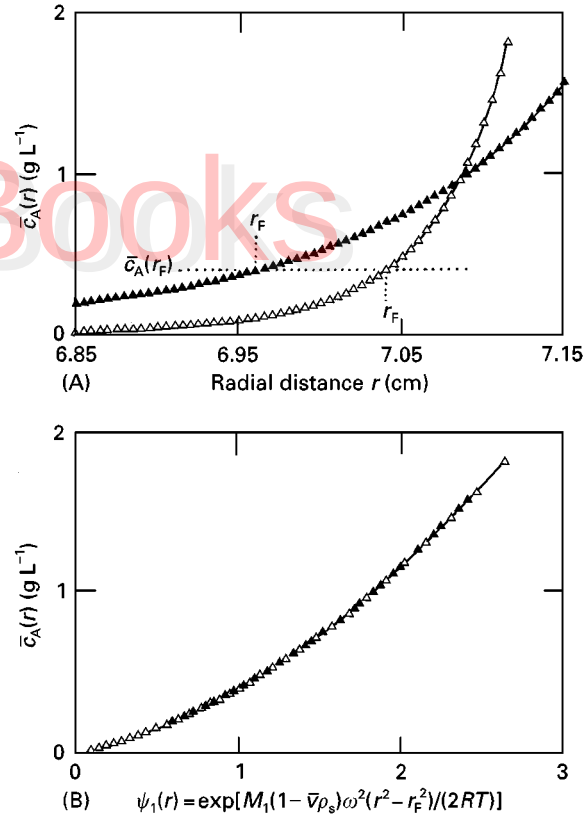

Figure 4 Studies of solute self-association by sedimentation equilibrium. (A) Simulated concentration distributions reflecting reversible dimerization of a monomer ($M_1 = 25$ kDa) governed by an association equilibrium constant of 3.5 L g^{-1} in sedimentation equilibrium experiments at 15 000 (▲) and 25 000 (△) rev min^{-1}. (B) Plot of data in readiness for global analysis according to eqn [15] with a fixed value of 0.4 g L^{-1} for the total solute concentration $\bar{c}_A(r_F)$ at reference radial position r_F.

DropBooks

distributions are at chemical equilibrium, the total solute concentration at each radial distance may be expressed in terms of monomer concentration by the relationship:

$$\bar{c}_A(r) = c_1(r) + K_2[c_1(r)]^2 \qquad [14]$$

On the other hand, the condition of sedimentation equilibrium dictates that the distribution of monomer be described by eqn [7]. Combination of these two requirements leads to the expression:

$$\bar{c}_A(r) = c_1(r_F)\psi_1(r) + K_2[c_1(r)\psi_1(r)]^2 \qquad [15]$$

$$\psi_1(r) = \exp[M_1(1 - \bar{\nu}_A\rho_s)\omega^2(r^2 - r_F^2)/(2RT)] \qquad [16]$$

The application of this approach is illustrated in **Figure 4B**, where global analysis of the two distributions from **Figure 4A** has been effected on the basis of a common $\bar{c}_A(r_F)$ value of 0.4 g L^{-1}, thereby ensuring a common value of $c_1(r_F)$. Magnitudes of $\psi_1(r)$ at 20°C have then been calculated on the basis of the appropriate r_F value, the buoyant molecular mass of monomer and the angular velocity. In as much as $c_1(r_F)$ and K_2 are both constants, their magnitudes are obtained by nonlinear curve-fitting of the combined $[\bar{c}_A(r), \psi_1(r)]$ data sets to the above quadratic expression in $\psi_1(r)$.

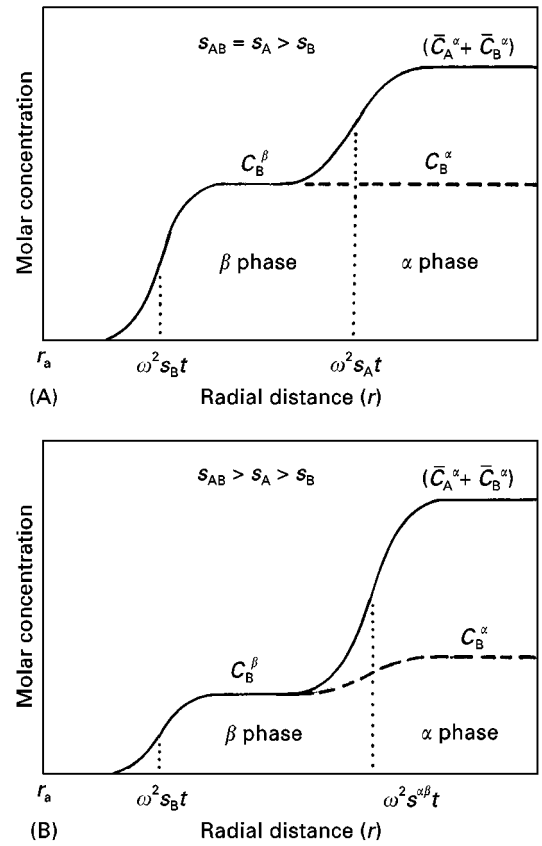

Figure 5 Schematic representations of boundary patterns encountered in sedimentation velocity studies of ligand binding. (A) Direct evaluation of the free ligand concentration (C_B^{α}) for a system where acceptor and acceptor–ligand complex(es) co-migrate. (B) The corresponding situation when acceptor and ligand are both macromelecular ($s_{AB} > s_A > s_B$).

Interactions Between Dissimilar Reactants

Although interactions between dissimilar reactants far outnumber those entailing solute self-association in biology, the study of ligand binding by analytical ultracentrifugation has received far less attention – a situation being remedied to some extent now.

Studies of Ligand Binding by Sedimentation Velocity

In considering the quantification of acceptor–ligand interactions by sedimentation velocity, there are two situations to examine: one in which a macromolecule (acceptor, A) reacts with a small molecule (ligand, *B*); and the situation in which both acceptor and ligand are macromolecular. In the former, provided that the ligand is sufficiently small for the acceptor–ligand complex *AB* (or complexes AB_i for ligand binding to multiple acceptor sites) to co-migrate with acceptor ($s_{AB} \cong s_A > s_B$), the free ligand concentration is readily determined by sedimentation velocity. As depicted schematically in **Figure 5A**, the subjection of an equilibrium mixture to a high centrifugal field under those circumstances generates a biphasic boundary pattern in which the concentration in the slower-migrating (β) phase reflects free ligand at its equilibrium concentration in the mixture (α phase) with total molar concentrations $\bar{C}_A^{\alpha}$ and $\bar{C}_B^{\alpha}$ of acceptor and ligand, respectively. Results obtained are thus akin to conventional ligand-binding data obtained by (say) equilibrium dialysis; and may therefore be treated in an analogous fashion.

In the second case in which the ligand is also macromolecular, the sedimentation coefficient of the *AB* complex is likely to be greater than that of either reactant ($s_{AB} > s_A > s_B$). Under those circumstances, a biphasic boundary pattern is again generated, but the slower-migrating phase corresponds to the reactant in molar excess: the situation represented in **Figure 5B** reflects a molar excess of ligand. Although the concentration of pure ligand in the slower-migrating phase (C_B^{β}) can be measured, it does not equal the free ligand concentration (C_B^{α}) in the equilibrium mixture. However for a 1 : 1 interaction, the free concentration of the other reactant may be

determined from the expression:

$$C_A^{\alpha} = (\bar{C}_A^{\alpha} - \bar{C}_B^{\alpha} + C_B^{\beta})(s^{\alpha\beta} - s_B)/(s_A - s_B) \quad [17]$$

where C_i again denotes a molar concentration, and where $s^{\alpha\beta}$ is the sedimentation coefficient of the reaction boundary between the pure solute phase and that corresponding to the original mixture. Combination of the consequent value of C_A^{α} with the composition of the mixture ($\bar{C}_A^{\alpha}$, $\bar{C}_B^{\alpha}$) then yields the binding constant K_{AB} on the grounds that:

$$K_{AB} = C_{AB}^{\alpha}/(C_A^{\alpha}C_B^{\alpha}) = (\bar{C}_A^{\alpha} - C_A^{\alpha})/[C_A^{\alpha}(\bar{C}_B^{\alpha} - \bar{C}_A^{\alpha} + C_A^{\alpha})] \quad [18]$$

For purposes of simplification, the above quantitative treatments assume migration in a rectangular cell under the influence of a homogeneous field. Sedimentation in a sector-shaped cell leads to radial dilution that slightly decreases the magnitudes of the various concentrations. However, the uncertainties inherent in the measurements of C_B^{β} and the various differences in sedimentation coefficients are usually sufficient to justify the approximations involved in such interpretation of sedimentation velocity patterns.

Studies of Ligand Binding by Sedimentation Equilibrium

For a reversible interacting between an acceptor *A* and a ligand *B*, there are only two independent sedimentation equilibrium distributions – one for the acceptor constituent which includes the acceptor contribution to *AB* complex(es) as well as free reactant; and the corresponding distribution for the ligand constituent. Thus:

$$\bar{C}_A(r) = C_A(r) + K_{AB}C_A(r)C_B(r) + \ldots \quad [19]$$

$$\bar{C}_B(r) = C_B(r) + K_{AB}C_A(r)C_B(r) + \ldots \quad [20]$$

Figure 6 presents sedimentation equilibrium distributions for the individual species in centrifugation of a 1 : 1 interacting system with $M_A(1 - \bar{\nu}_A\rho_s) = 12$ kDa, $M_B(1 - \bar{\nu}_B\rho_s) = 3$ kDa and $K_{AB} = 50\,000$ mol L^{-1} at 15 000 rpm. Also shown are the constituent distributions.

Substituting the condition of sedimentation equilibrium (eqn [7]) for the individual reactants into the above expressions allows them to be rewritten in the form:

$$\bar{C}_A(r) = C_A(r_F)\psi_A(r) + K_{AB}C_A(r_F)C_B(r_F)\psi_A(r)\psi_B(r) + \ldots \quad [21]$$

$$\bar{C}_B(r) = C_B(r_F)\psi_B(r) + K_{AB}C_A(r_F)C_B(r_F)\psi_A(r)\psi_B(r) + \ldots \quad [22]$$

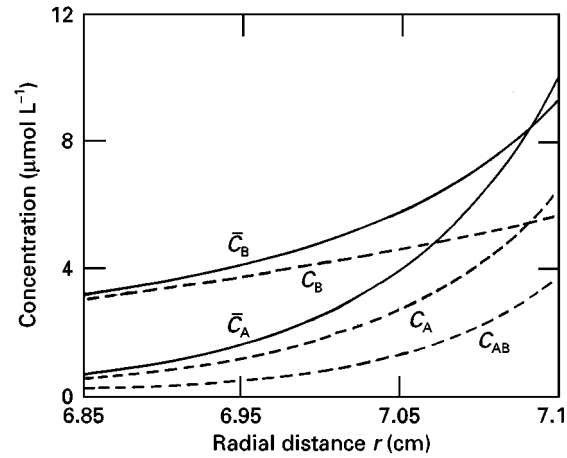

Figure 6 Simulated sedimentation equilibrium distributions for the individual species (- - -) resulting from centrifugation at 15 000 rpm of a mixture of acceptor with $M_A(1 - \bar{\nu}_A\rho_s) = 12$ kDa and ligand with $M_B(1 - \bar{\nu}_B\rho_s) = 3$ kDa undergoing reversible 1 : 1 interaction governed by a binding constant of 50 000 mol L^{-1}. The solid curves describe distributions in terms of the total concentrations of the separate constituents ($\bar{C}_A$, $\bar{C}_B$).

Furthermore, because $\psi_A(r) = [\psi_B(r)]^u$ where $u = [M_A(1 - \bar{\nu}_A\rho_s)]/[M_B(1 - \bar{\nu}_B\rho_s)]$, these expressions become discrete polynomials in terms of $\psi_B(r)$ and the constant parameters $C_A(r_F)$, $C_B(r_F)$ and K_{AB}. The problem of evaluating K_{AB} thus amounts to nonlinear regression analysis of the [C_i, $\psi_B(r)$] distributions to obtain the three constants as curve-fitting parameters.

The extent to which advantage may be taken of this approach clearly depends upon the nature and number of sedimentation equilibrium distributions available for analysis. In that regard, the maximum potential for quantitative analysis pertains to the situation in which the optical system provides information on the separate concentrations of acceptor and ligand constituents. However, the optical system may well only monitor one constituent, or it may yield a single distribution related to the combined constituent concentrations, $\bar{C}_A(r) + \bar{C}_B(r)$. The latter situations are clearly less than optimal from the viewpoint of characterizing the interactions, but procedures (admittedly less accurate) have been devised to illustrate the feasibility of a quantitative analysis, even under these adverse circumstances.

Future Developments

Despite the fact that the characterization of macromolecular interactions by analytical ultracentrifugation has attracted the attention of physical biochemists for the past 50 years, its application is only now filtering through to the general biochemical community. Inasmuch as the required methodology is

DropBooks

largely in place, the stage seems set for an exciting revitalization of analytical ultracentrifugation as the cell biologists begin to tackle the characterization of the myriads on interactions detected during the past few decades of qualitative research.

See also: **II/Centrifugation:** Analytical Centrifugation, Theory.

Further Reading

Fujita H (1962) *Mathematical Theory of Sedimentation Analysis*. New York: Academic Press.

Harding SE and Winzor DJ (2000) Sedimentation velocity analytical ultracentrifugation as a probe for ligand binding. In: Harding SE and Chowdry PZ (eds). *Protein–Ligand Interactions*: *A Practical Approach*. Oxford: IRL Press.

Harding SE, Rowe AJ and Horton JC (eds) (1992) *Analytical Ultracentrifugation in Biochemistry and Polymer Science*. Cambridge: Royal Society of Chemistry.

Nichol LW and Winzor DJ (1972) *Migration of Interacting Systems*. Oxford: Clarendon Press.

Schachman HK (1959) *Ultracentrifugation in Biochemistry*. New York: Academic Press.

Schuster TM and Laue TM (eds) (1994) *Modern Analytical Ultracentrifugation*: *Acquisition and Interpretation of Data for Biological and Synthetic Polymer Systems*. Boston: Birkhäuser.

Svedberg T and Pedersen KO (1940) *The Ultracentrifuge*. Oxford: Clarendon Press

Williams JW (ed.) (1963) *Analytical Ultracentrifugation in Theory and Experiment*. New York: Academic Press.

Wills PR, Jacobsen MP and Winzor DJ (1997) Direct analysis of sedimentation equilibrium distributions reflecting macromolecular interactions. *Progress in Colloid and Polymer Science* 107: 1–10.

Winzor DJ and Harding SE (2000) Sedimentation equilibrium in the analytical ultracentrifuge as a probe of ligand binding. In: Harding SE and Chowdry PZ (eds) *Protein–Ligand Interactions*: *A Practical Approach*. Oxford: IRL Press.

Preparative Centrifugation

See **II/CENTRIFUGATION/Large-Scale Centrifugation**

Theory of Centrifugation

A. G. Letki, Alfa Laval, Warminster, PA, USA

Copyright © 2000 Academic Press

Introduction

Separation

Separation, as discussed here, is a mechanical means of the following:

- Separating immiscible liquids with different specific gravities (purification).
- Removing insoluble solids from a liquid (clarification if a liquid is the main product; dewatering if the solids are the chief product).
- Removing excess liquid from insoluble solids (thickening with the solids slurry in a more viscous form being the product).
- Some intermediate combination (degritting – removal of oversize particles; desliming – removal of fine particles; or some other form of classification – splitting the slurry into two generally liquid components with the solids being split based on particle size and/or density).

Centrifuges

Centrifuges are usually divided into two types, sedimenting and filtering. Sedimenting centrifuges are characterized by a solid bowl wall and include tubular bowl (**Figure 1**), disc stack (**Figure 2**) decanter (**Figure 3**) and imperforate basket centrifuges. Filtering centrifuges have perforated bowl walls, which support screens or cloth or both and include perforate basket centrifuges, peelers and pushers.

The ultracentrifuge and the gas centrifuge represent special cases that establish separations based on gradients on a molecular scale and are not included in this discussion.

Although centrifuges have been applied industrially for well over a century, centrifuge theory is not well developed. Centrifuges are not designed for specific applications using fundamental principles. Any discussion of centrifuge theory must also define the limitation of the theory. The best means of predicting the performance that will be obtained by processing a material through a centrifuge is to actually process the material through a centrifuge.